Insect Biochemistry and Molecular Biology 106 (2019) 19–27

Contents lists available at ScienceDirect

Insect Biochemistry and Molecular Biology

journal homepage: www.elsevier.com/locate/ibmb

Fibroinase and its physiological inhibitors involved in the regulation of silk gland development in the silkworm, *Bombyx mori*

Pengchao Guo[a,b,1], Zhan Wang[a,1], Qian Wang[a], Huawei Liu[a], Yunshi Zhang[a], Haiyang Xu[a], Ping Zhao[a,b,*]

[a] State Key Laboratory of Silkworm Genome Biology, Southwest University, Chongqing, 400715, China
[b] Chongqing Key Laboratory of Sericultural Science, Chongqing engineering and Technology Research Center for Novel Silk Materials, Southwest University, Chongqing, 400715, China

ARTICLE INFO

Keywords:
Cathepsin L-like cysteine protease
Enzymatic activity
Enzyme and its inhibitors
Silk gland development

ABSTRACT

Fibroinase, a cathepsin L-like cysteine protease, was previously identified in the silk gland of the silkworm, *Bombyx mori*. It shows high degradation activity during the pre-pupa period, when the silk gland undergoes apoptosis and remodeling. Here, we recombinantly expressed pro-fibroinase and activated it *in vitro*. Fibroinase showed optimal hydrolytic activity at pH 4.0 and its optimum temperature was about 42 °C. One physiological inhibitor, *B. mori* cysteine protease inhibitor (BCPI) was found, which showed strong inhibitory activity against fibroinase. The inhibitory reaction was caused by the formation of a non-covalent complex; this is in contrast to a previously reported mode of fibroinase inhibition by Serpin18. Expression profiles and immunolocalization analysis demonstrated that fibroinase was involved in silk gland development by degrading silk proteins and apoptosis/remodeling of silk glands at specific points. Furthermore, the comparison of the temporal expression of fibroinase and its inhibitors, BCPI and Serpin18, indicated that these inhibitors were involved in the silk gland development by regulating the activity of fibroinase from the fifth instar until the early spinning stage. These findings improve our understanding of the mechanism of protease regulation and its inhibitors in silk gland development.

1. Introduction

Cysteine proteases are present in almost all living organisms, and are mainly responsible for catabolism and protein processing. In addition, cysteine proteases are involved in apoptosis and extracellular matrix remodeling (Chapman et al., 1997). Lysosomal cathepsins, which are involved in the degradation and reconstruction of tissues, are the most abundant group of cysteine proteases (Fonovic and Turk, 2014). Since the discovery of cathepsin C in *Homo sapiens* in the 1940s, many more cathepsins, named cathepsin A to cathepsin Z, have been identified (Chen et al., 2004; Schreuder et al., 2014; Turk et al., 1996; Wang et al., 2011). In 1990, a cathepsin L-like cysteine protease was purified from silkworm eggs and named BCP (*Bombyx mori* Cysteine Protease); it was found to hydrolyze vitellogenin in an acidic environment *in vitro* (Kageyama and Takahashi, 1990). In addition to their eggs, BCP was identified in silkworm fat bodies, oocytes, the hemolymph, and other areas. (Yamamoto et al., 2000). In 1993, another cathepsin L-like cysteine protease was identified in the degenerating silk glands of silkworms in the pre-pupa period that displayed hydrolytic activity against fibroin *in vitro*; thus, it was named fibroinase (Sumida et al., 1993). Localization analysis showed that fibroinase was expressed in the lumen of the silk gland and silk gland cells at the fourth, fifth instar, and pre-pupa stages (Watanabe et al., 2004a); natural fibroinase was first purified from silk glands during the fourth instar and fourth molt (Watanabe et al., 2004b). Further research found that fibroinase also showed hydrolytic activity towards sericin; thus, it is also considered a cathepsin L-like protease in the silk gland of the silkworm (Watanabe et al., 2007). Possible roles of fibroinase in the silk gland were then speculated, including the digestion of proteins and organelles in lysosomes, as well as the digestion of the unnecessary fibroin and sericin that accumulated in the lumen of the silk gland (Watanabe et al., 2006). Zhong et al. found that silk protein degradation and silk gland remodeling/apoptosis occurred almost simultaneously during the larval-pupa stage (Zhong et al., 2005). Our previous results showed that fibroinase was weakly detected at the fifth instar stage and mainly observed in the spinning period in the silk gland,

* Corresponding author. State Key Laboratory of Silkworm Genome Biology, Southwest University, Chongqing, 400715, China.
E-mail address: zhaop@swu.edu.cn (P. Zhao).
[1] Both authors contributed equally to this work.

https://doi.org/10.1016/j.ibmb.2019.01.003
Received 16 October 2018; Received in revised form 22 December 2018; Accepted 9 January 2019
Available online 10 January 2019
0965-1748/

which consistent with the degradation function of fibroinase in the silk gland (Guo et al., 2015). In addition, it was shown that cathepsin activity is required for posterior silk gland destruction and timely pupation, and that cathepsin inhibitors like *B. mori* cysteine protease inhibitor (BCPI) and E-64D (an irreversible membrane-permeable inhibitor of cysteine protease) could prevent the destruction process in the posterior silk gland (Ma et al., 2013). These findings indicated that fibroinase participates in the silk gland apoptosis during silk gland development, and that its activity is regulated by inhibitors.

To functionally characterize fibroinase and understand its mechanism of activity and regulation by inhibitors in silk gland development, we recombinantly expressed fibroinase and determined its physiological inhibitors in the silk gland. Expression profiles and immunolocalization analysis of fibroinase demonstrated that fibroinase was involved in silk gland development. Furthermore, the comparison of the temporal expression of fibroinase and its inhibitors indicated that complementary inhibitors regulated the activity of fibroinase in the process of silk gland development.

2. Materials and methods

2.1. Bioinformatics analysis

The full-length cDNA sequence (NM_001043999.2) and protein sequence (NP_001037464.2) of the *B. mori* fibroinase precursor (pro-fibroinase) were obtained from NCBI. Characteristic and sequence analysis of pro-fibroinase were performed using the ExPASy server (http://www.expasy.org/), SMART analysis service (http://smart.embl-heidelberg.de/) and ClustalX 1.8.

2.2. Expression of fibroinase in Pichia pastoris

The open reading frame of pro-fibroinase without the signal peptide was amplified by PCR using silk gland cDNA (strain p50, Dazao) from pre-pupa silkworms as the template, then the PCR products were ligated into the pPICZαA vector between EcoRI and NotI. The recombinant plasmid was linearized with SacI (Takara Bio, Shiga, Japan) and electroporated into Pichia pastoris strain GS115. Then, successful clones were selected using a low concentration of Bleomycin (100 μg/mL) on YPD plates. Thereafter, high-productivity clones were selected from YPD plates using a high concentration of Bleomycin (1000 μg/mL).

One of the selected clones was inoculated in BMGY medium in a baffled flask and incubated at 28 °C until the culture reached an optical density at 600 nm (OD600) of 5.0. The BMGY medium was centrifuged at room temperature and the supernatant was removed; transfected cells were then suspended in BMMY medium at 28 °C until they grew to an OD600 = 1.0 in a new baffled flask to induce expression. Next, 1% methanol added to the culture and 1% culture was collected every 24 h; the optimal time of induction was determined through western blotting (Anti-fibroinase) of the culture at different time points. After centrifuging the culture at the optimal induction time, the supernatant was harvested for protein purification.

2.3. Activation and purification of fibroinase

Harvested supernatant was adjusted to pH 6.8 with 1 M Tris-HCl buffer (pH 8.5) and loaded onto a HiTrap nickel-chelating column (GE Healthcare, Little Chalfont, UK) equilibrated with binding buffer (20 mM Tris-HCl, 200 mM NaCl, pH 6.8). The fibroinase was eluted with elution buffer (20 mM Tris-HCl, 200 mM NaCl, 300 mM imidazole, pH 6.8) and then loaded onto a PD-10 desalting column (GE Healthcare) equilibrated with reaction buffer (20 mM NaAc, 50 mM NaCl, pH 4.2). After elution with reaction buffer and activation at 25 °C for 100–120 min, the solution was loaded onto a HiLoad 16/60 Superdex 75 column (GE Healthcare) equilibrated with reaction buffer. SDS-PAGE was performed on the purified fibroinase, which was then stored at −80 °C for further analysis.

2.4. Activity assays of fibroinase and its inhibitors

Activity assays were performed as described previously (Sutthikhum et al., 2004) using Z-Phe-Arg-MCA (Peptide Institute Inc., Osaka, Japan) as substrate (Barrett and Kirschke, 1981). BCPI (NP_001037057.1) was purified as described previously (Hou et al., 2016). The highest activity in each experiment was defined as 100%. To determine the effect of pH on fibroinase hydrolytic activity, a 200 μL reaction system containing 0.05 μg fibroinase, 0.1 mM substrate and 40 mM Britton-Robinson's buffer (pH 2.0–10.0) was prepared, and samples were incubated for 10 min at 25 °C. The thermal stability of fibroinase was performed by measuring its activity from 16 to 70 °C in a 200 μL reaction system containing 20 mM reaction buffer (pH 4.2), 0.05 μg fibroinase and 0.1 mM substrate, then reaction was stopped by adding 40 μL stopping buffer (300 mM monochloro acetic acid). The kinetic parameters, K_m and V_{max}, were determined at 25 °C in a 200 μL assay mixture, which contains 20 mM reaction buffer (pH 4.2), 0.05 μg fibroinase, and the indicated concentrations of substrate. K_m and V_{max} were calculated using a double reciprocal plot.

An inhibitory activity assay was performed in a 200 μL reaction mixture containing 20 mM reaction buffer (pH 4.2), 0.05 μg fibroinase, 2.5 μg BCPI, and 0.1 mM substrate. After incubation for 10 min at 25 °C, the reaction was performed by adding substrate and the intensity of the fluorescence signal was measured using the GloMax-Multi Detection System Photometer (Promega, Madison, WI, USA) at an excitation wavelength of 360 nm and an emission wavelength of 450 nm. As a standard, 2000 fluorescence units represented 1 μM fluorogenic substrate was hydrolyzed (Sutthikhum et al., 2004). The inhibitory constant K_i was determined by adding various concentrations of BCPI to a 200 μL reaction system. The K_i value was calculated with GraphPad Prism 5.0 using the following formula (Copeland, 2000):

$$y = V_0 \times \left(1 - \frac{E_t + x + \left(K_i\left(1 + \frac{S}{K_m}\right)\right) - \sqrt{(E_t + x+)\left(K_i\left(1 + \frac{S}{K_m}\right)\right)^2 - 4 \times E_t \times x}}{2 \times E_t}\right)$$

where E_t is the concentration of fibroinase (nM), S is the concentration of Z-Phe-Arg-MCA (nM), K_m is the kinetics parameter of fibroinase toward Z-Phe-Arg-MCA, and V_0 is the relative activity (%) when BCPI was not added.

To observe the interactions of BCPI with fibroinase, various concentrations of BCPI were incubated with 1 μg fibroinase in 15 μL reaction buffer at 25 °C for 15 min. The mixture was subjected to SDS-PAGE, followed by alkaline Native-PAGE (Davis, 1964). The activity of the proteins is retained in an alkaline Native-PAGE (pH 8.3), which separates proteins based on their specific charge (charge-to-mass ratio). The SDS-PAGE and alkaline Native-PAGE products were analyzed by Coomassie brilliant blue staining and western blotting, respectively. BCPI, fibroinase, and fibroinase incubated with 10 μM E-64D (a commercial irreversible inhibitor that inactivates cysteine proteases by binding to the active site (Cys) of the protease and forming a covalent-binding complex) served as controls. After SDS-PAGE or Native-PAGE, proteins were transferred to PVDF membranes using the Trans-Blot Turbo Transfer System (Bio-Rad Laboratories, Hercules, CA, USA), and the PVDF membranes were sequentially incubated with primary antibody and secondary antibody after blocking. The primary antibodies used were rabbit anti-fibroinase or rabbit anti-BCPI, which were prepared using recombinant pro-fibroinase or BCPI, and the secondary antibody

was HRP-labeled Goat Anti-Rabbit IgG (Beyotime, Jiangsu, China). Next, the PVDF membranes were incubated with SuperSignal West Femto Maximum Sensitivity Substrate (Thermo Fisher Scientific, Waltham, MA, USA) and observed in a ChemiScope 3300 mini (Clinx Science Instruments, Shanghai, China).

2.5. Silkworm feeding and materials collection

Silkworms (strain p50, Dazao) were maintained in the State Key Laboratory of the Silkworm Genome Biology Laboratory (Southwest University, China), and were bred routinely with a diet of mulberry leaves at 25 ± 1 °C with 70 ± 5% humidity. Silk glands at different stages of development were dissected on ice and frozen in liquid nitrogen immediately for further bioassays. In this study, nineteen representative time points were chosen: the second molt stage (L2Mt), day 0 of third instar (L3D0), day 2 of third instar (L3D2), third molt stage (L3Mt), day 0 of fourth instar (L4D0), day 2 of fourth instar (L4D2), day 3 of fourth instar (L4D3), fourth molt stage (L4Mt), day 0 of fifth instar (L5D0), day 1 of fifth instar (L5D1), day 3 of fifth instar (L5D3), day 5 of fifth instar (L5D5), day 7 of fifth instar (L5D7), wandering stage (WaSt), day 1 of spinning stage (SpD1), 12 h into the spinning stage (SpH12), day 2 of spinning stage (SpD1), 36 h into the spinning stage (SpH36), and day 3 of spinning stage (SpD1).

2.6. RT-qPCR and western blot analysis

RNA was extracted using TRIZOL reagent (Invitrogen, Carlsbad, CA, USA) and then stored at −80 °C. All cDNA samples were obtained using M-MLV reverse transcriptase (Invitrogen) at 42 °C and stored at −80 °C. The cDNA samples were normalized using *B. mori sw22934* as an internal control. RT-qPCR primers were designed and are presented in the supplementary materials (Table S1). Three independent replicates were performed for each RT-qPCR experiment.

Protein samples were extracted from homogenized silk glands using lysis buffer (8 M Urea, 25 mM DTT, 30 mM Chaps). All protein samples were centrifuged at 13,000 × *g* for 15 min at 4 °C, and the supernatants (extracted proteins) were collected for western bolt analysis. Western blotting was performed as described above, and all extracted proteins were normalized using *B. mori* α-tubulin as an internal control. Except for rabbit anti-α-tubulin IgG (Beyotime), the primary antibodies—rabbit anti-fibroinase, rabbit anti-BCPI, and rabbit anti-Serpin18—were prepared using recombinant pro-fibroinase, BCPI and Serpin18, respectively. HRP-labeled goat anti-rabbit IgG (Beyotime) was used as a secondary antibody.

2.7. Immunolocalization analysis

The silk glands of silkworms at different development stages (seven representative time points were chosen) were dissected and divided into anterior silk gland (ASG), middle silk gland (MSG), and posterior silk gland (PSG). This segmentation method was chosen based on a previous report (Dong et al., 2016). The three fragments were embedded in O.C.T. Compound (Sakura, Alphen aan den Rijn, Netherlands) and stored at −80 °C. The embedded fragments were cross-sectioned into 7–10-μm slices at −30 °C using the CryoStar NX50 Freeze Slicer (Thermo Fisher Scientific) and attached to a glass slide as the immunolocalization sample.

Samples were fixed with 4% paraformaldehyde Fix Solution (BBI Life science, Shanghai, China) for 10 min and washed with PBST (PBS with 0.3% Triton-X100, pH 7.4) three times. Then, the samples were blocked with blocking buffer (PBS with 1% BSA and 10% goat serum) for 1 h and incubated with primary antibody solution (PBS with 1% BSA and 0.1% rabbit anti-fibroinase IgG, or PBS with 1% BSA as a negative control). After washing with PBST three times, samples were incubated with secondary antibody solution (PBS with 1% BSA and 0.2% Cy3-labeled goat anti-rabbit IgG) for 2 h and washed again. The samples were then incubated with DAPI Staining Solution (Beyotime) for 10 min and washed with PBS three times. Next, glass slides were prepared with the Antifade Mounting Medium (Beyotime), covered with a coverslip, and observed using the EVOS FL Auto Imaging System (Thermo Fisher Scientific).

3. Results

3.1. Fibroinase sequence analysis

The pro-fibroinase gene encodes a protein containing 341 amino acids with a signal peptide composed of 16 amino acids; this indicates that fibroinase might be secreted into the extracellular matrix. The molecular weight of pro-fibroinase is 38.1 kDa and its theoretical pI was 5.9. In addition to the signal peptide, pro-fibroinase contains an inhibitor_I29 region and a cysteine protease region (Supplementary Fig. S1A). BLAST analysis revealed that pro-fibroinase shares ~51–78% identity with cysteine proteases from other Lepidoptera species. In addition to the high similarity with other cathepsin L-like cysteine proteases, the pro-domain of pro-fibroinase contains two ERYNIN and KNYD motifs, both of which are characteristic of cathepsin L (Karrer et al., 1993) (Supplementary Fig. S1B). Moreover, the GCNGG structural motif, as well as an important SPV motif related to secretion, were located at the C-terminus (Chauhan et al., 1998; Karrer et al., 1993), and the Cys–His–Asn triad at the active site was identified in mature fibroinase (Supplementary Fig. S1B). These characteristics suggested that fibroinase is a typical cathepsin L-like cysteine protease with optimal function at a lower pI. Furthermore, the N-terminus of the papain family cysteine protease region was predicted to be LPEQVDWRKHGA, consistent with the results of fibroinase N-terminal sequencing (Sutthikhum et al., 2004).

3.2. Fibroinase expression and activation

To express fibroinase *in vitro*, we cloned the *fibroinase* gene into pPICZαA and expressed it in *P. pastoris*. One clone with high productivity was selected from several different clones and the amount of protein produced was measured at different time points. As shown in Fig. 1A, pro-fibroinase was expressed after incubation for 24 h and reached maximal expression between 72 h and 96 h, suggesting that 72 h after induction is the optimal time of expression. After induction for 72 h, pro-fibroinase was purified by affinity chromatography and was activated in reaction buffer. Activation automatically occurred at a lower pH. As shown in Figs. 1B and 100–120 min appeared to be the best time for activation. During the activation process, six bands were observed between the bands corresponding to pro-fibroinase and fibroinase20 min after activation (Fig. 1B, lane 3), indicating that the six bands were intermediate forms during automatic activation. Thereafter, fibroinase was further purified by gel filtration chromatography (Fig. 1C) and the purity of the eluted protein was estimated through SDS-PAGE (Fig. 1D). Gel filtration analysis indicated that the eluted fibroinase had a molecular mass of 26 kDa, approximately consistent with its theoretical molecular mass of 27.0 kDa. This finding indicated that fibroinase exists as a monomer in solution. The yield of pro-fibroinase and fibroinase during the purification process is shown in the supplementary materials (Table S2).

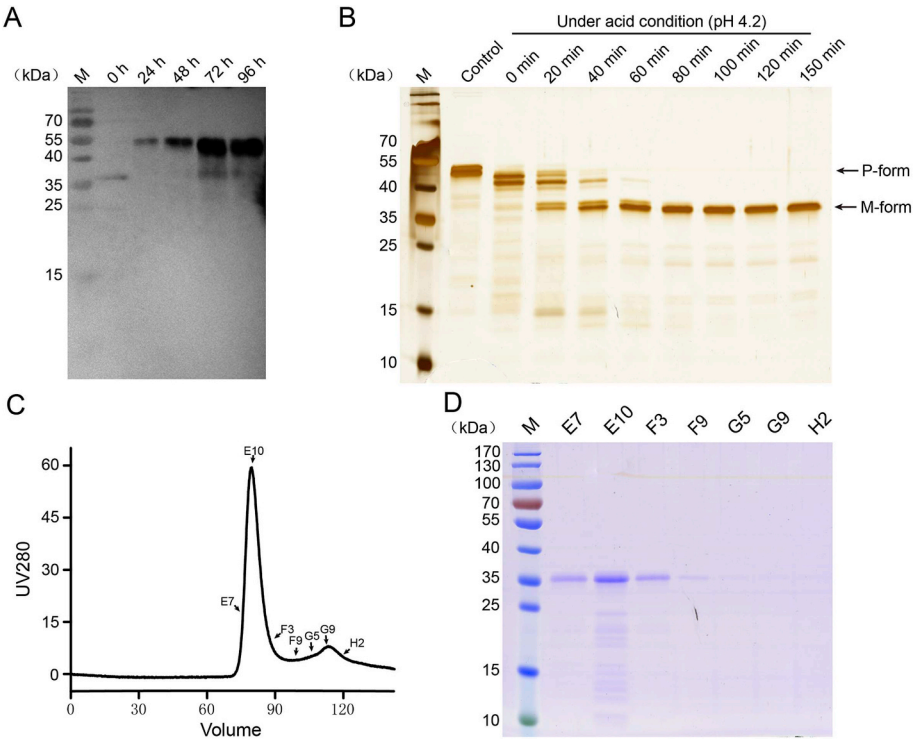

Fig. 1. Expression and purification of fibroinase. (A) The detection of fibroinase expression with western blot. M: marker. (B) Auto-activation of pro-fibroinase. M: marker; P-form: pro-fibroinase; M-form: fibroinase. (C) and (D) Purification of fibroinase by gel filtration and SDS-PAGE analysis. Lanes E7 to H2: different check points of the elution in gel filtration.

3.3. Enzymatic properties of fibroinase

To determine the biochemical properties of fibroinase, its hydrolytic activity was tested at a pH range of 2.0–10.0. The maximum activity was observed at pH 4.0 (Fig. 2A). Notably, the activity was hard to detect at pH > 6.0. With a longer incubation time or/and higher concentration, fibroinase showed weak hydrolyzing activity at a pH range of 6.0–7.0 (Fig. S2). This suggested that fibroinase can only function in acidic and neutral conditions. The effect of temperature on fibroinase activity was investigated at a range of 16–70 °C (Fig. 2B). The reaction rate increased with temperature from 16 to 42 °C, then gradually declined at higher temperatures. The plot showed a bell-like shape with the highest activity at 42 °C. When the temperature dropped to 16 °C, activity decreased by more than 60%, while no activity was detected at 60 °C or higher as a result of enzyme denaturation. Notably, the activity of fibroinase at physiological temperature (28 °C) decreased to 50% of its maximum activity. Furthermore, the kinetics parameters of fibroinase toward the substrate, Z-Phe-Arg-MCA, were determined and calculated using a double reciprocal plot (Fig. 2C). The K_m value was 9.13 μM and V_{max} value was 16.39 nM/s.

3.4. BCPI is one of physiological inhibitor of fibroinase

In a previous study, BCPI was proved to be a strong and specific inhibitor of cathepsin L-like cysteine proteases (Kurata et al., 2001; Ma et al., 2013). Additionally, both fibroinase and BCPI were previously identified in the silk glands at the fifth instar larval and spinning stages (Dong et al., 2016). The spatiotemporal distribution of BCPI and fibroinase suggest that BCPI might be a physiological inhibitor of fibroinase, in addition to Serpin 18, which has already been demonstrated to be a physiological inhibitor of fibroinase at the fifth instar (Guo et al., 2015). To determine whether BCPI would inactivate fibroinase, we expressed and purified recombinant BCPI, and then tested its inhibitory activity against fibroinase. As shown in Fig. 3A, BCPI showed significant inhibitory activity against fibroinase; at a mass ratio of 50:1 (BCPI to fibroinase), the proteolysis activity of fibroinase showed a reduction of almost 100% compared to the control. BCPI inhibited proteolysis activity in a dose-dependent manner, and the extrapolated molar ratio of inhibitor-to-protease was approximately 1.2 (Fig. 3B). Furthermore, inhibitory kinetic behavior was determined, and the Ki parameter was calculated to be 8.74 pM. These results demonstrated that BCPI acted as a potential inhibitor of fibroinase.

To elucidate how BCPI inhibits fibroinase activity, a reaction solution of fibroinase and BCPI was analyzed using SDS-PAGE and alkaline Native-PAGE (Fig. 3). The apparent molecular weight of the fibroinase-BCPI complex was predicted to be 38.8 kDa, but no corresponding band was detected by either Coomassie brilliant blue staining or western blot analysis under denatured conditions (Fig. 3C). However, under natural conditions, additional bands were observed after incubating fibroinase with different concentrations of BCPI; these bands were bound by anti-BCPI antibody and anti-fibroinase antibody during western blot analysis (Fig. 3D, lanes 3–6). Moreover, the additional bands were further confirmed by liquid chromatography-tandem mass spectrometry (LC-MS/MS), and both the high-confidence unique peptides of BCPI and fibroinase were detected (Fig. S3), implying that BCPI interacts with fibroinase and forms a non-covalent complex.

3.5. Expression patterns of fibroinase and its physiological inhibitors in silk glands

To investigate the role of fibroinase in silk gland development in *B. mori*, the expression patterns of fibroinase and its physiological inhibitors, BCPI and Serpin 18, were analyzed at the transcript and protein level from L2Mt to SpD3 in silkworm larvae. As shown as in Fig. 4, fibroinase was mainly expressed during molt periods, day 0 of each instar (newly exuviated larva), the wandering stage, and the spinning stage at both the transcript and protein levels. The increase and/or decrease in fibroinase expression were similar to the profiles of the

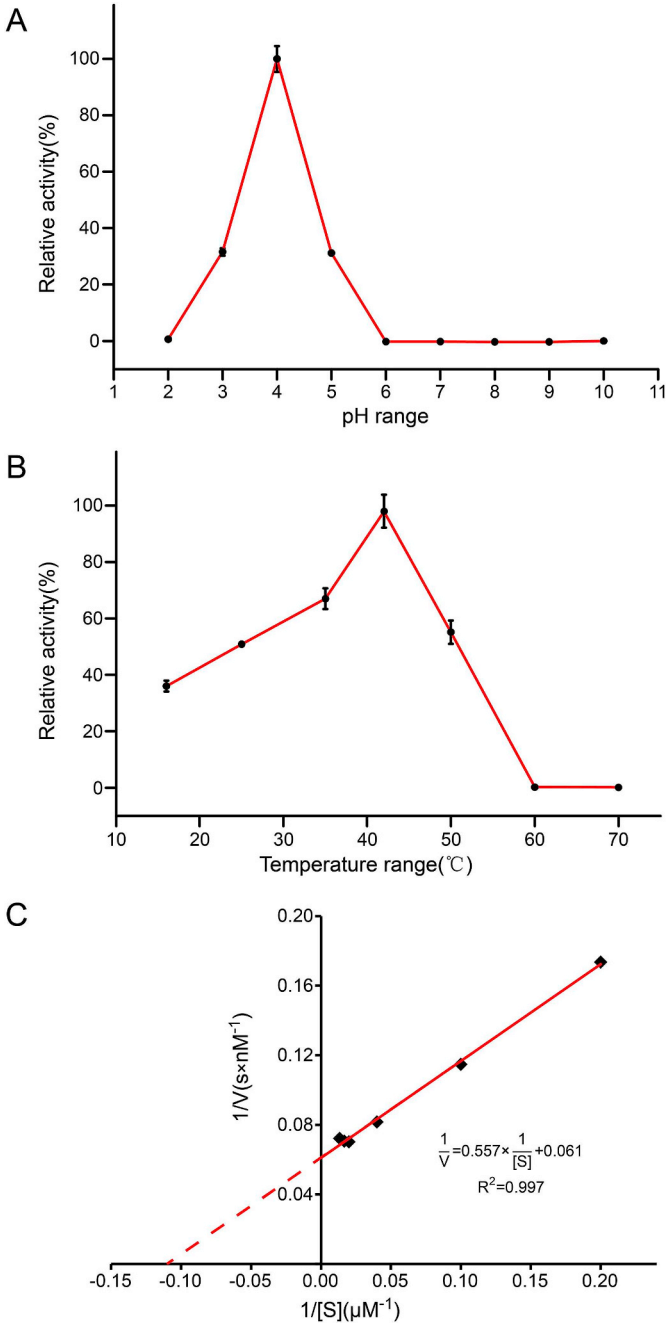

Fig. 2. The enzymatic properties of fibroinase toward Z-Phe-Arg-MCA. (A) The effect of pH on hydrolytic activity of fibroinase. (B) The hydrolysis of fibroinase at different temperature. (C) Determination of kinetics parameters of fibroinase toward fluorogenic substrate, Z-Phe-Arg-MCA. Each point represents mean values from three independent tests.

remodeling and/or apoptosis of silk glands, indicating that fibroinase is a key enzyme in silk gland development. However, we found that fibroinase protein was minimally expressed at the early fifth instar larval stage, but showed increased expression at the late fifth instar, inconsistent with the transcript level. This might be because fibroinase was reversibly bound to Serpin 18 in a Michaelis-like complex that was degraded into small fragments by free fibroinase; thus, the amount of both fibroinase and Serpin 18 were decreased (Guo et al., 2015).

Serpin 18 was only synthesized during the fifth instar and showed the same expression patterns at the transcript and protein levels: an increase from the first to fifth day, a decrease on the seventh day, and no expression by the wandering stage. BCPI transcript was found to be expressed in the fifth instar, wandering stage, and the early spinning stage, and showed a similar pattern to that of fibroinase from L4Mt to L5D5 (Fig. 4D). However, BCPI protein was only observed at the end of the fifth instar and early spinning stage (from L5D5 to WaSt). That means when Serpin 18 expression decreased and disappeared at the end of the fifth instar, BCPI expression increased to fill the gap and prevent excessive fibroinase hydrolytic activity during the late fifth instar and early spinning stages. Moreover, BCPI and Serpin 18 were not detected before the fifth instar, showing that they mainly affected fibroinase activity from the fifth instar until the early spinning stage.

To further confirm the expression patterns of fibroinase in different sections of the silk gland, we chose several representative time points of silk gland development to perform immunolocalization analysis (Fig. 5A and Supplementary Fig. S4): L4D3 (before molt, with spinning), L4Mt (molt stage), L5D0 (after molt, without spinning and feeding), L5D3 (feeding period, without spinning), L5D7 (feeding period, with synthesis of fibroin and sericin), SpH12 (spinning stage, without feeding), and SpH36 (end of spinning, pre-pupa stage). As shown in Fig. 5A, fibroinase expression was detected in both cell layers and the lumen, and was usually found in the cell layers of the silk gland and secreted into the silk gland cavity at specific stages, especially those in which the apoptosis and remodeling of the silk gland occurred, such as L4Mt, L5D0, and SpH36. These findings indicated that fibroinase plays an important role in the digestion of residual silk proteins during silk gland development. In addition, there were different expression patterns for fibroinase in ASG, MSG, and PSG: in ASG, fibroinase (red fluorescence) could be detected in the lumen during larval spinning stages such as L4D3 and SpH12; in MSG, red fluorescence was observed in the lumen during stages when sericin was not intensively synthesized and/or stored, such as L4Mt, L5D0, L5D3 and SpH36; in PSG, fibroinase signal distribution was similar to that of MSG, and a stronger red fluorescence signal was detected on the side of the cell layers further from the cavity. These findings suggested that fibroinase has different expression patterns in ASG, MSG, and PSG, indicating that fibroinase plays different physiological roles in different segments of the silk gland. Fibroinase is secreted in ASG to prevent the lumen from blocking during spinning, while it is responsible for degrading excess and unnecessary fibroin and sericin in the lumen of MSG and PSG when silk proteins are not needed.

To explore the localization of BCPI in the silk gland, we selected two representative time points based on the BCPI expression pattern at the protein level, L5D7 and SpH12, to perform immunolocalization (Fig. 5B and Supplementary Fig. S5). The results showed that BCPI was detected in the cell layers of ASG, MSG, and PSG at L5D7 and SpH12, while a weak fluorescence signal was observed in the lumen of silk glands, indicating that BCPI was secreted to prevent the degradation of silk gland tissue and fibroin and/or sericin proteins in the lumen.

4. Discussion

4.1. Fibroinase is a cathepsin L-like protease and its activity is inactivated by BCPI

It is known that cathepsin is synthesized as an inactive precursor containing a pro-domain, which normally blocks substrate binding to the active site and plays an important role in protein folding and intracellular sorting (Coulombe et al., 1996; Pandey et al., 2004, 2009). In a previous study, the pro-domain of a similar cathepsin L-like protease, BCP, was shown to be related to the correct folding of the enzyme, and was removed after auto-activation (Takahashi et al., 1997; Yamamoto et al., 1999). Therefore, we expressed pro-fibroinase in P. pastoris and successfully activated it. We also successfully expressed fibroinase using the same method, but its expression was very low and the protein was unstable during the purification process (data not known). By contrast, pro-fibroinase was highly stable in binding buffer at 4 °C for 96 h during purification.

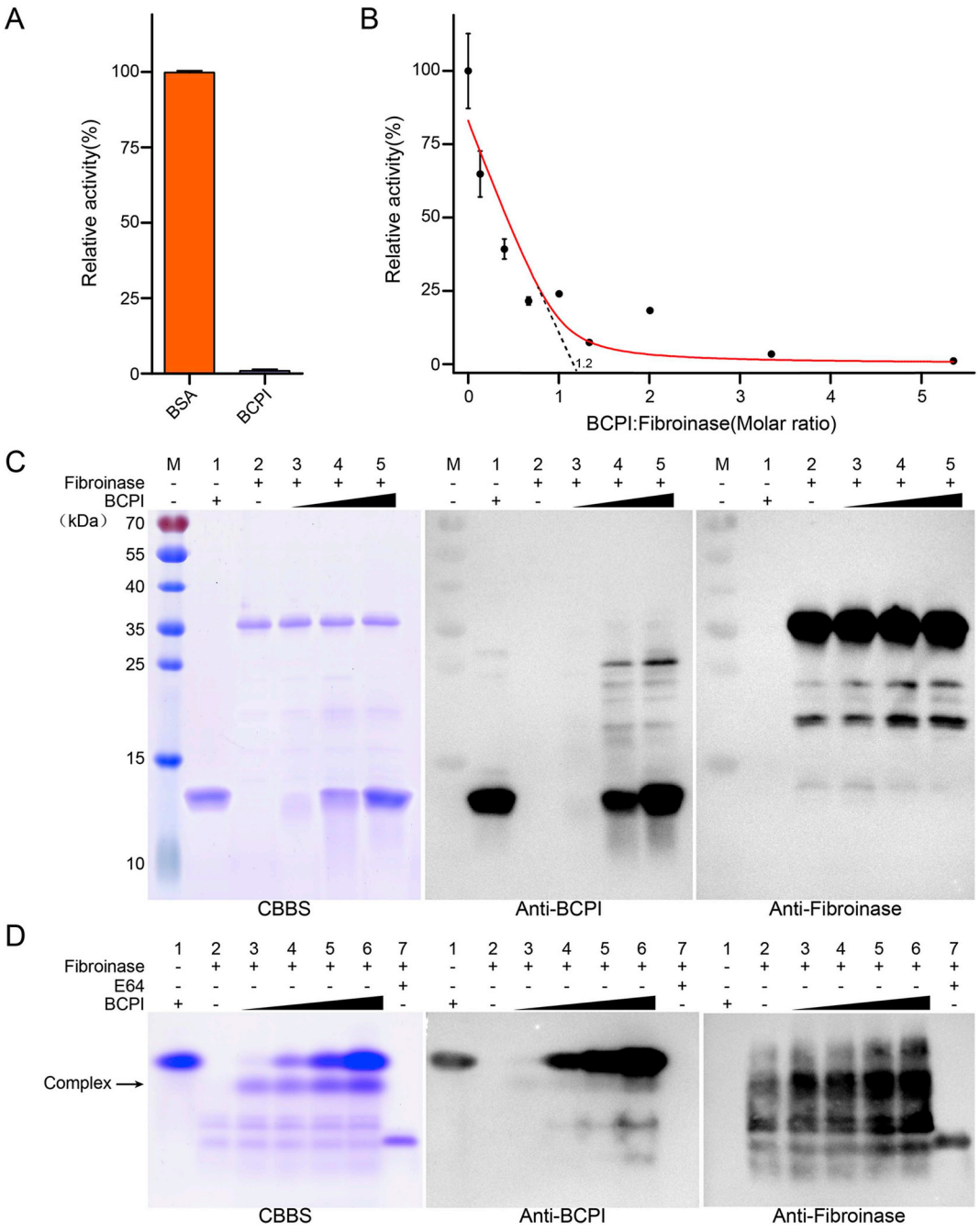

Fig. 3. Inhibitory activity of BCPI towards fibroinase. (A) The bar graph diagrams of residual activity of fibroinase incubated with BSA (Control) and BCPI. (B) Measurement of K_i of BCPI with fibroinase. (C) Analysis of interaction between BCPI and fibroinase using the SDS-PAGE. M: marker; Lane 1: 2 μg BCPI; Lane 2: 1 μg fibroinase; Lanes 3 to 5: 0.5 μg, 2 μg, 4 μg BCPI with 1 μg fibroinase; CBBS: Coomassie brilliant blue staining. (D) Analysis of interaction between BCPI and fibroinase using the alkaline Native-PAGE. Lane 1: 2 μg BCPI; Lane 2: 1 μg fibroinase; Lanes 3 to 6: 0.5 μg, 1 μg, 2 μg, 4 μg BCPI with 1 μg fibroinase; Lane 7: 1 μg fibroinase with 10 μM E-64; CBBS: Coomassie brilliant blue staining.

In this study, BCPI was identified as a strong and reversible inhibitor of fibroinase (Fig. 3). Sequence analysis indicated that BCPI contains an inhibitor_I29 domain, which is very similar to the inhibitor_I29 region in the prodomain of pro-fibroinase (Supplementary Fig. S1A) (Groves et al., 1996). This finding suggested that BCPI might interact with fibroinase and inhibit its enzyme activity by preventing the binding of the substrate to the active site. In the interaction between BCPI and fibroinase, no band corresponding to the fibroinase-BCPI complex was detected under denatured conditions (Fig. 3C). In contrast, western blotting and LC-MC/MC analyses of proteins subjected to Native-PAGE confirmed that fibroinase interacted with BCPI and formed a non-covalent complex. Our previous studies showed that Serpin 18, a high-molecular-weight cysteine protease inhibitor, can also inactivate fibroinase. However, Serpin 18 inhibits fibroinase through a different mechanism: by forming an unstable Michaelis-like complex; the complex is then degraded into small fragments by free fibroinase (Guo et al., 2015).

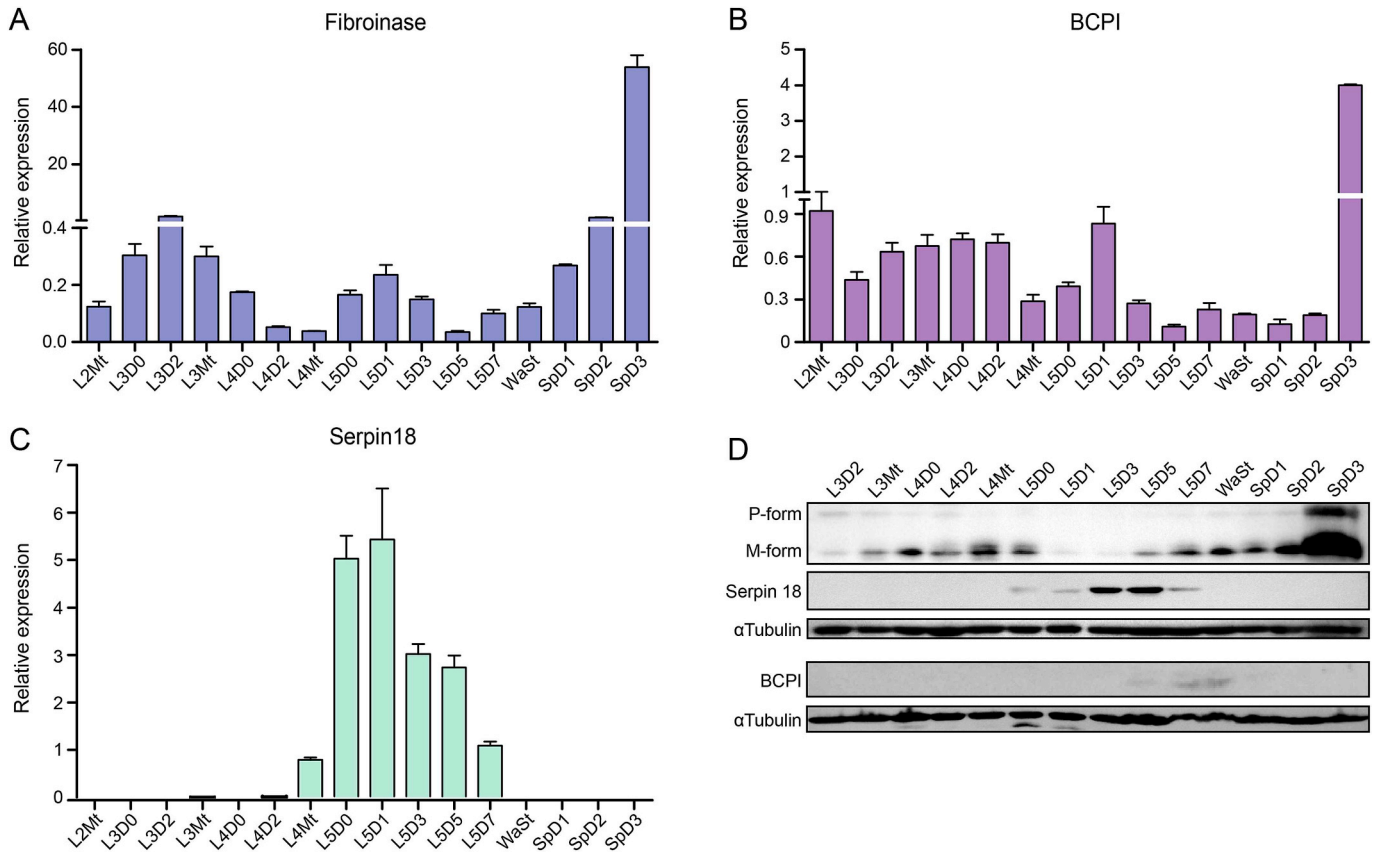

Fig. 4. Expression patterns of fibroinase, Serpin18 and BCPI in the silk gland. Expression patterns of (A) fibroinase, (B) BCPI and (C) Serpin18 at transcription level from L2Mt to SpD3. (D) Expression patterns of fibroinase, BCPI and Serpin18 at protein level from L2Mt to SpD3. P-form: pro-fibroinase. M-form: fibroinase.

4.2. Fibroinase and its inhibitors are involved in the regulation of silk gland development

According to the results of RT-qPCR, western blot, and immunolocalization, fibroinase was highly expressed during molt periods, day 0 of each instar (newly exuviated larva), and late spinning stages. This periodic expression pattern of fibroinase is correlated to silk gland development, such as silk gland remodeling and/or degradation, as well as the digestion of unnecessary fibroin and sericin in the silk gland lumen during the molt stage and late spinning stage. Moreover, we found that fibroinase might play different roles in ASG, MSG, and PSG. In ASG, fibroinase mainly prevented blockage of the lumen by sericin during spinning. In MSG and PSG, it degraded unnecessary sericin and fibroin proteins in the lumen. These results demonstrated that fibroinase is involved in the digestion of sericin and fibroin in the lumen, and in apoptosis within the silk gland. We also investigated the location and expression profile of the physiological inhibitors of fibroinase. Our previous study found that Serpin 18 was located in the cell layers and the lumen of silk glands (Guo et al., 2015). Similarly, BCPI was located in the cell layers and in the lumen of silk glands (Fig. 5B), suggesting that they may prevent the degradation of silk gland tissue, fibroin, and sericin in the lumen. The temporal expression profile showed that Serpin 18 was only synthesized in fifth instar larvae, while BCPI was expressed in the fifth instar, wandering stage, and early spinning stage (Fig. 4D). These two inhibitors were present from L5D0 to SpD1, which is a critical period for silk protein synthesis and storage. Their expression patterns explain why fibroinase was expressed during this period but did not affect silk gland development. Therefore, it is believed that Serpin 18 and BCPI, the physiological inhibitors of fibroinase, are involved in silk gland development by regulating the activity of fibroinase from the fifth instar until the early spinning stage. We also found that BCPI expression rapidly increased at SpD3 at the transcriptional level (Fig. 4B) because the activity of fibroinase was necessary for silk gland degradation at SpD3; however, this expression pattern was not observed at the protein level (Fig. 4D), possibly due to delayed expression between the translational and transcriptional levels.

Outside of physiological inhibitors, the natural pH within the silk gland may also impact silk gland development by affecting fibroinase activity. Our activity assay showed that recombinant fibroinase displayed the highest activity under acidic conditions (pH 3–5), minimal activity in a neutral environment (pH 7), and almost no activity under alkaline conditions. Moreover, native fibroinase also showed weak hydrolyzation activity towards fibroins in a neutral environment (pH 7) (Sumida et al., 1993). Using a pH-sensitive dye, Miyake and Azuma observed that the MSG was acidic (pH 5–6) and that the PSG was neutral (pH 7–8) in feeding larvae (day 1–7 of fifth instar larvae); furthermore, they found that the pH value changed from acidic (pH ~5–6) to neutral (pH ~7) in MSG of spinning larvae (Miyake and Azuma, 2008). Similarly, Domigan. et al. measured the intraluminal pH range of the silk gland lumen in *B. mori* and found that the pH range of the silk gland was 6.2–6.5 (ASG), 7 (MSG), and 8 (PSG) in fifth instar larvae at the spinning stage (Domigan et al., 2015). These findings suggested that fibroinase activity would be lost during the spinning stage, consistent with the decrease in the expression of inhibitors during the spinning period without affecting silk gland development. These results also indicated that pH might be another factor regulating the activity of fibroinase in vivo, which is an effective supplement to inhibitor activity.

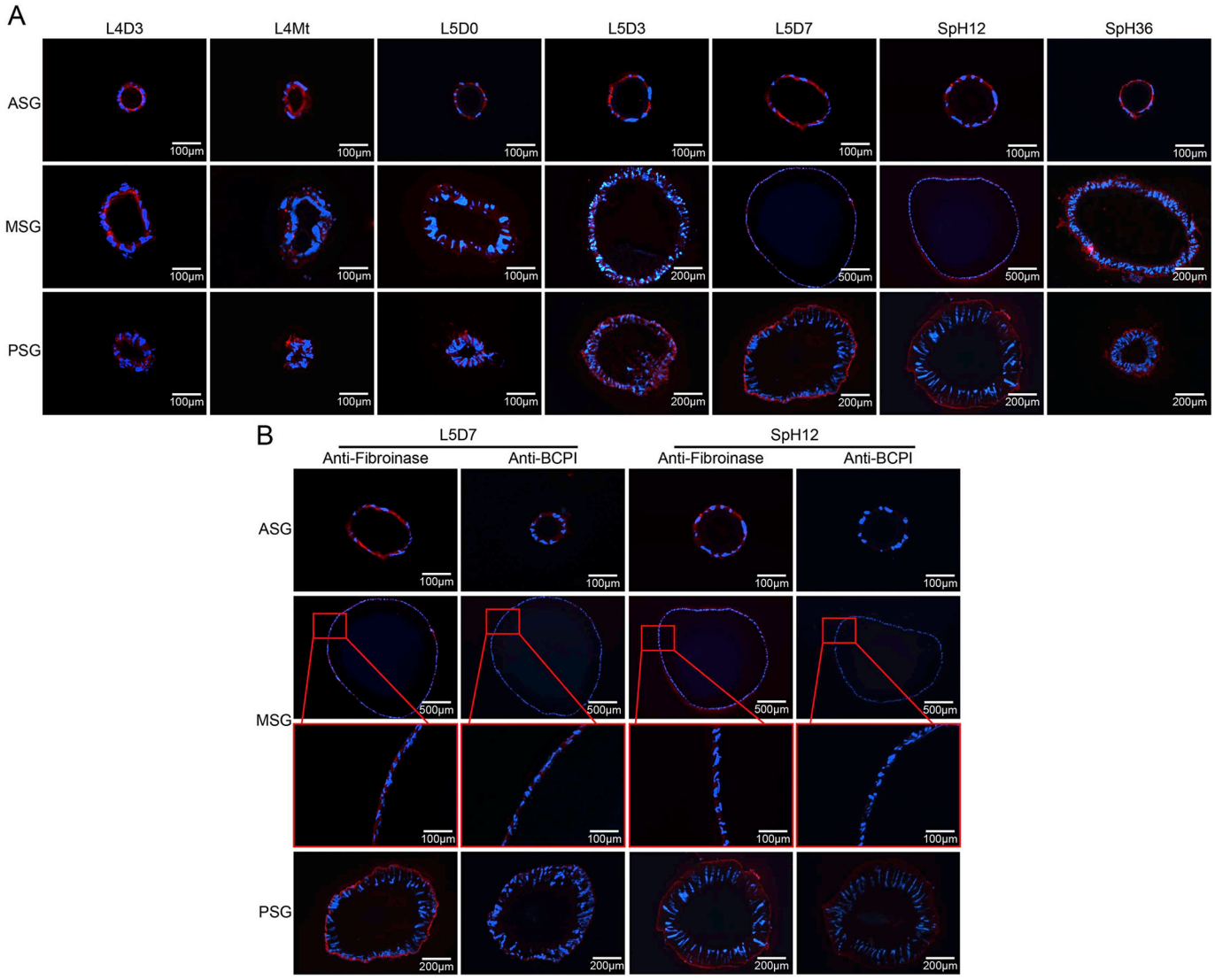

Fig. 5. Localization of fibroinase and BCPI in the silk gland. (A) Immunolocalization of fibroinase in silk gland at L4D3, L4Mt, L5D0, L5D3, L5D7, SpH12 and SpH36. (B) Immunolocalization of fibroinase and BCPI in silk gland at L5D7 and SpH12.

Acknowledgments

We are grateful to all the developers of ClustalX and Expasy. This work was supported by the National Natural Science Foundation of China (31502019), Chongqing Research Program of Basic Research and Frontier Technology (CSTC, 2015jcyjA10072), the Fundamental Research Funds for the Central Universities (XDJK2018C012) and the 2017 Special Grants Program for National Cocoon Silk Development (No. GJ2017JSB001).

Appendix A. Supplementary data

Supplementary data to this article can be found online at https://doi.org/10.1016/j.ibmb.2019.01.003.

References

Barrett, A.J., Kirschke, H., 1981. Cathepsin B, cathepsin H, and cathepsin L. Methods Enzymol. 80 Pt C, 535–561.
Chapman, H.A., Riese, R.J., Shi, G.P., 1997. Emerging roles for cysteine proteases in human biology. Annu. Rev. Physiol. 59, 63–88.
Chauhan, S.S., Ray, D., Kane, S.E., Willingham, M.C., Gottesman, M.M., 1998. Involvement of carboxy-terminal amino acids in secretion of human lysosomal protease cathepsin L. Biochemistry 37, 8584–8594.
Chen, L.Z., Zhou, J.L., Zhou, Y.Z., Gong, H.Y., Li, P.Y., 2004. Molecular cloning of two Rhipicephalus haemaphysaloides haemaphysaloides cathepsin L-like cysteine proteinase gene. Chin. J. Biotechnol. 20, 203–208.
Copeland, R.A., 2000. Enzymes. A Practical Introduction to Structure, Mechanism, and Data Analysis, second ed. Wiley-VCH, New York.
Coulombe, R., Grochulski, P., Sivaraman, J., Menard, R., Mort, J.S., Cygler, M., 1996. Structure of human procathepsin L reveals the molecular basis of inhibition by the prosegment. EMBO J. 15, 5492–5503.
Davis, B.J., 1964. Disc electrophoresis. Ii. Method and application to human serum proteins. Ann. N. Y. Acad. Sci. 121, 404–427.
Domigan, L.J., Andersson, M., Alberti, K.A., Chesler, M., Xu, Q., Johansson, J., Rising, A., Kaplan, D.L., 2015. Carbonic anhydrase generates a pH gradient in Bombyx mori silk glands. Insect Biochem. Mol. Biol. 65, 100–106.
Dong, Z., Zhao, P., Zhang, Y., Song, Q., Zhang, X., Guo, P., Wang, D., Xia, Q., 2016. Analysis of proteome dynamics inside the silk gland lumen of Bombyx mori. Sci. Rep. 6, 21158.
Fonovic, M., Turk, B., 2014. Cysteine cathepsins and extracellular matrix degradation. Biochim. Biophys. Acta 1840, 2560–2570.
Groves, M.R., Taylor, M.A.J., Scott, M., Cummings, N.J., Pickersgill, R.W., Jenkins, J.A., 1996. The prosequence of procaricain forms an alpha-helical domain that prevents access to the substrate-binding cleft. Structure 4, 1193–1203.
Guo, P.C., Dong, Z., Zhao, P., Zhang, Y., He, H., Tan, X., Zhang, W., Xia, Q., 2015. Structural insights into the unique inhibitory mechanism of the silkworm protease inhibitor serpin18. Sci. Rep. 5, 11863.
Hou, Y., Yang, H., Li, J., Gong, J., Zhou, X., Tian, S., Guo, C., Xia, Q., 2016. Cloning and expression analysis of cysteine proteinase inhibitor gene (bcpi) in silkworm (Bombyx mori). Journal of Agricultural Biotechnology 24, 1915–1924.

Kageyama, T., Takahashi, S.Y., 1990. Purification and characterization of a cysteine proteinase from silkworm eggs. Eur. J. Biochem. 193, 203–210.
Karrer, K.M., Peiffer, S.L., DiTomas, M.E., 1993. Two distinct gene subfamilies within the family of cysteine protease genes. Proc. Natl. Acad. Sci. U. S. A. 90, 3063–3067.
Kurata, M., Yamamoto, Y., Watabe, S., Makino, Y., Ogawa, K., Takahashi, S.Y., 2001. Bombyx cysteine proteinase inhibitor (BCPI) homologous to propeptide regions of cysteine proteinases is a strong, selective inhibitor of cathepsin L-like cysteine proteinases. J. Biochem. 130, 857–863.
Ma, L., Liu, S., Shi, M., Chen, X.X., Li, S., 2013. Ras1CA-upregulated BCPI inhibits cathepsin activity to prevent tissue destruction of the Bombyx posterior silk gland. J. Proteome Res. 12, 1924–1934.
Miyake, S., Azuma, M., 2008. Acidification of the silk gland lumen in Bombyx mori and Samia cynthia ricini and localization of H + -translocating vacuolar-type ATPase. J. Insect Biotechnol. Sericol. 77, 9–16.
Pandey, K.C., Barkan, D.T., Sali, A., Rosenthal, P.J., 2009. Regulatory elements within the prodomain of Falcipain-2, a cysteine protease of the malaria parasite Plasmodium falciparum. PLoS One 4, e5694.
Pandey, K.C., Sijwali, P.S., Singh, A., Na, B.K., Rosenthal, P.J., 2004. Independent intramolecular mediators of folding, activity, and inhibition for the Plasmodium falciparum cysteine protease falcipain-2. J. Biol. Chem. 279, 3484–3491.
Schreuder, H.A., Liesum, A., Kroll, K., Bohnisch, B., Buning, C., Ruf, S., Sadowski, T., 2014. Crystal structure of cathepsin A, a novel target for the treatment of cardiovascular diseases. Biochem. Biophys. Res. Commun. 445, 451–456.
Sumida, M., Takimoto, S., Ukai, M., Matsubara, F., 1993. Occurrence of fibroinase in degenerating silk gland in the pharate adult of the silkworm, Bombyx-mori. Comp. Biochem. Physiol. B 105, 239–245.
Sutthikhum, V., Watanabe, M., Sumida, M., 2004. Fibroinase activity in Bombyx mori silk gland in the larval-pupal development and its partial purification from spinning larva. J. Insect Biotechnol. Sericol. 73, 71–79.
Takahashi, S.Y., Yamamoto, Y., Watabe, S., Kageyama, T., 1997. Autolytic activation mechanism of Bombyx acid cysteine protease (BCP). Biochem. Mol. Biol. Int. 42, 591–600.
Turk, D., Podobnik, M., Kuhelj, R., Dolinar, M., Turk, V., 1996. Crystal structures of human procathepsin B at 3.2 and 3.3 Angstroms resolution reveal an interaction motif between a papain-like cysteine protease and its propeptide. FEBS Lett. 384, 211–214.
Wang, G., Peng, D., Sun, J., Huang, W., Peng, H., Long, H., 2011. Cloning and sequence analysis of a new cathepsin L-like cysteine proteinase gene from Ditylenchus destructor. Chin. J. Biotechnol. 27, 60–68.
Watanabe, M., Fujii, S., Miyata, S., Sumida, M., 2004a. Localization of fibroinase in the silk gland of domesticated silkworm, Bombyx mori, wild silkmoths, Samia cynthia ricini and Antheraea pernyi studied by confocal laser scanning microscopy. Int. J. WILD SILKMOTH SILK 9, 1–14.
Watanabe, M., Kamei, K., Sumida, M., 2006. Fibroinase activity of silk gland in larval and early pupal development of the silkworm, Bombyx mori assayed with a fluorescent quenched peptide substrate. J. Insect Biotechnol. Sericol. 75.
Watanabe, M., Kamei, K., Sumida, M., 2007. Sericin digestion by fibroinase, a cathepsin L-like cysteine proteinase, of Bombyx mori silk gland. J. Insect Biotechnol. Sericol. 76, 9–15.
Watanabe, M., Yura, A., Yamanaka, M., Kamei, K., Hara, S., Sumida, M., 2004b. Purification and characterization of fibroinase, a cathepsin L-like cysteine proteinase, from the silk gland in the fourth instar Bombyx mori larva at the fourth molt period, stage D2. J. Insect Biotechnol. Sericol. 73, 61–70.
Yamamoto, Y., Watabe, S., Kageyama, T., Takahashi, S.Y., 1999. Proregion of Bombyx mori cysteine proteinase functions as an intramolecular chaperone to promote proper folding of the mature enzyme. Arch. Insect Biochem. Physiol. 42, 167–178.
Yamamoto, Y., Yamahama, Y., Katou, K., Watabe, S., Takahashi, S.Y., 2000. Bombyx acid cysteine protease (BCP): hormonal regulation of biosynthesis and accumulation in the ovary. J. Insect Physiol. 46, 783–791.
Zhong, Y., Zeng, L., Huang, Z., Liu, J., Deng, X., Yang, W., Cao, Y., Gu, S., 2005. Characteristics of degeneration and apoptosis of silk gland during the larval-pupal metamorphosis in the silkworm, Bombyx mori. Acta Entomol. Sin. 48, 319–324.